

submitted to Ap.J.

Kinematics of Black Hole X-ray Binary GRS 1915+105

V. Dhawan

National Radio Astronomy Observatory, Socorro, NM 87801 USA.

vdhawan@nrao.edu

I. F. Mirabel ¹*European Southern Observatory, Casilla 19001, Santiago 19, Chile*

fmirabel@eso.org

M. Ribó

*Departament d'Astronomia i Meteorologia, Universitat de Barcelona,
Martí i Franques 1, 08028 Barcelona, Spain*

mribo@am.ub.es

I. Rodrigues

Universidade do Vale do Paraíba, Sao Jose dos Campos, Brazil

irapuan@if.ufrgs.br

ABSTRACT

The space velocity of a stellar black hole encodes the history of its formation and evolution. Here we measure the 3-dimensional motion of the microquasar GRS 1915+105, using a decade of astrometry with the NRAO Very Long Baseline Array, together with the published radial velocity. The velocity in the Galactic Plane deviates from circular rotation by $53\text{--}80\pm 8\text{ km s}^{-1}$, where the range covers any specific distance from 6–12 kpc. Perpendicular to the plane, the velocity is only $10\pm 4\text{ km s}^{-1}$. The peculiar velocity is minimized at a distance 9–10 kpc, and is then nearly in the radial direction towards the Galactic Center. We discuss

¹On leave from Service d'Astrophysique, CEA-Saclay, 91191 Gif-sur-Yvette, France.

mechanisms for the origin of the peculiar velocity, and conclude that it is most likely a consequence of Galactic velocity diffusion on this old binary, rather than the result of a supernova kick during the formation of the $14 M_{\odot}$ black hole. Finally, a brief comparison is made with 4 other BH binaries whose kinematics are well determined.

Subject headings: astrometry — stars: kinematics — stars: individual (GRS 1915+105) — techniques: high angular resolution — techniques: interferometric

1. Introduction

GRS 1915+105 is a famous microquasar with superluminal ejecta (Mirabel & Rodriguez 1994), and spectacular X-ray variability from an unstable accretion disk (Greiner et al. 1996; Belloni et al. 2000). For nearly a decade, its nature was highly obscured at a distance D of ~ 10 kpc. Finally, IR spectroscopy with the VLT (Greiner et al. 2001) was used to measure the heliocentric radial velocity of -3 ± 10 km s $^{-1}$ for the center of mass of the binary, a mass of $14 \pm 4 M_{\odot}$ for the compact object, with a donor mass of $\sim 1.2 \pm 0.2 M_{\odot}$ in an orbit of 33.5 days period. VLBA imaging (Dhawan et al. 2000a), in addition to the ejecta during outbursts, revealed an AU-sized radio jet closely coupled to the accretion disk activity. Under the conditions imaged here, the so-called low-hard state, the flux of the AU-size jet follows the variation in X-rays with a time-lag of a few minutes, (Mirabel et al. 1998; Dhawan et al. 2000a). The jet is hence located within 1 AU (0.1 mas) of the black hole.

2. Observations and Results

2.1. Observations

Our observations spanned ~ 10 years, sampled at random times dictated by the flare activity of the source. Usually the goal was to image the AU-size jet and larger scale superluminal ejecta in coordination with X-ray instruments. The moving ejecta can confuse the position determination. Indeed there were some occasions just after a major flare when the central nucleus was very weak or absent, and the moving ejecta dominated the flux density of the source. We have hence selected for this astrometric study only those images which were dominated by the central source of flux density 10 to 50 mJy, corresponding to the AU-size flat-spectrum nuclear jet. Examples of images are published in Dhawan et al. (2000a); Fuchs et al. (2003); Ribó et al. (2004); Miller-Jones et al. (2007).

Standard VLBA phase-referencing was used, (Beasley & Conway 1995) with a total cycle time of 3 minutes, of which 1 minute was on the primary calibrator J1924+1540, at a separation of 5.3° from the target. This technique provides the position of the black hole relative to the reference source, whose position has been pre-determined in the ICRF frame. Most of the observations were at a frequency of 8.4 GHz (3.6cm wavelength). During some observations, depending on the radio spectra, (if available from monitoring with other instruments) we observed at 3.6 and 2 cm. These were alternated every 20min, at 256Mbit s^{-1} recording. Standard post-processing corrections were applied for ionospheric refraction using a GPS-based global model. A-priori amplitude calibration was done from measured system temperatures and antenna gains, followed by self-calibration on the reference source, application of the refined calibration to all sources including the target, and imaging.

We fitted a single elliptical Gaussian to each image to extract the position. The formal errors of the fit are far exceeded by tropospheric variations, resulting in position errors ~ 1 mas *rms* at each epoch. The earliest observations have larger error due to the poor choice of reference sources, J1922+1530 (4.8° away, but quite resolved) and J1925+2106, 10.5° away from the target. We estimated the errors, including systematic errors peculiar to the weather on that day, from the scatter in image position over intervals of ~ 20 min. In later observations, a second calibrator, J1922+0840 (2.9° away), was observed as a quality check and processed in identical fashion to the target. Positions at the two wavelengths on a given observation date agreed, and were averaged together for that date. On one occasion observations were possible on successive days, positions from which were averaged together.

2.2. Results

The measurements ¹ are summarized in Table-1 and Figure-1, showing the coordinates of the black hole versus time. We fit the following position and proper motion at MJD 51545 (01 January 2000):

$$\begin{aligned} \text{RA (J2000)} & 19^{\text{h}}15^{\text{m}}11^{\text{s}}.54902 \pm 0.7 \text{ mas} & \text{Dec(J2000)} & +10^\circ 56' 44'' .7478 \pm 0.9 \text{ mas} \\ \mu_{\text{RA}} \text{ Cos(Dec)} & = -2.86 \pm 0.07 \text{ mas yr}^{-1} & \mu_{\text{Dec}} & = -6.20 \pm 0.09 \text{ mas yr}^{-1} \end{aligned}$$

¹Strictly, the measured VLBA positions are Geocentric. In the table, plot & fit, we report measured quantities, rather than correcting them for parallax with an uncertain distance. In the fit for proper motion, the error is reduced by the random observation date, and the long timespan. The parallax is 0.1 mas at $D=10$ kpc. The changes in proper motion if we correct for parallax are $\sim 0.01 \text{ mas yr}^{-1}$, far below our measurement errors. Thus Geocentric positions can safely be taken as Heliocentric.

The corresponding Heliocentric motions in Galactic coordinates are:

$$\mu_l = -6.82 \pm 0.10 \text{ mas yr}^{-1} \quad \mu_b = -0.35 \pm 0.07 \text{ mas yr}^{-1}$$

Using our measured proper motion and the known V_{radial} of $-3 \pm 10 \text{ km s}^{-1}$, we transform these measured Heliocentric quantities with the standard method of Johnson & Soderblom (1987) updated for J2000, and the Solar peculiar motion measured by Hipparcos, [U_{\odot} , V_{\odot} , $W_{\odot} = 10.0, 5.25, 7.17 \text{ km s}^{-1}$] from Dehnen & Binney (1998). We use the convention U + toward $l = 0^\circ$; V + toward $l = 90^\circ$; W + toward the North Galactic Pole.

We compare these measured velocities with those expected from circular rotation at 220 km s^{-1} at the location of the black hole. For the distance, 11 to 12 kpc have been proposed, (Fender 2003; Dhawan et al. 2000b), but since considerably smaller values are suggested by others, e.g. Kaiser et al. (2004), we let the distance be a free parameter in Figure 2 and Table 2. We then evaluate the velocity discrepancy in local and Galactocentric frames, and note that:

- The measured W component is small, so the black hole velocity lies primarily in the Galactic Plane.
- At any distance there is a significant component of measured velocity directed inward to the Galactic Center, whereas none is expected for purely circular motion.
- The extremum (negative) proper motion from Galactic rotation along this line of sight occurs at $D = 9 \text{ kpc}$, and is $-5.85 \text{ mas yr}^{-1}$, while $-6.82 \text{ mas yr}^{-1}$ is measured.
- Figure 3 shows that the total peculiar velocity of the black hole (in either LSR or GC frame) is minimized at $D = 9\text{--}10 \text{ kpc}$, and is then 53 km s^{-1} in the radial direction towards the Galactic Center.
- The measured heliocentric velocity matches that expected from circular rotation at $\sim 12 \text{ kpc}$, as already noted by Greiner et al. (2001). However, at this distance, the total peculiar velocity is 83 km s^{-1} .
- At $D = 6.5 \text{ kpc}$, both the Galactocentric components mismatch circular rotation by over 45 km s^{-1} each.

Hence, the distance favoured by velocity matching is 9–10 kpc, but this is not a very strong argument. A distance determined by trigonometric parallax, while possible with the VLBA, remains very challenging for this object.

2.3. The Galactocentric Orbit

We next compute the Galactocentric orbit of the black hole assuming a smooth Galactic potential composed of disk, spheroid and halo, following Johnston et al. (1995). Figure 4 shows the orbit assuming a distance of 12 kpc. The path for the past 1 Gyr is the blue (dashed) line, with the last 250 Myr in red (solid line). The orbit deviates from circularity with an eccentricity of 0.285, and reaches a maximum height above the Galactic Plane of only 230 pc, typical of the thin disk population. However, GRS 1915+105 does not match the velocity of thin disk objects at any distance. Detailed computation of the orbit including the effects of spiral arms is beyond the scope of this paper.

3. Discussion

We discuss mechanisms by which the black hole could have acquired its anomalous velocity. To summarize, though the velocity is significant, its component out of the Galactic plane is low, so an impulsive origin cannot be proved. The age and uncertain distance of the system disallow a strong conclusion about the origin of the velocity. However, our data helps to rank the probability of three mechanisms.

3.1. Stellar Diffusion

An individual star in the disk can acquire significant changes in angular momentum from non-axisymmetric forces such as spiral arms, leading to an increase of its non-circular motion with age (Weilen 1977; Sellwood & Binney 2002). If we assume the binary is as old as the donor, a red giant of $1.2 M_{\odot}$ aged ~ 4 Gyr, then it has endured about 16 Galactic orbits. Velocity imparted by spiral arm passages conforms naturally to the measured low velocity perpendicular to the Galactic plane, and has had sufficient time to operate, given the age of the system. In comparison, the non-circular velocity of progressively older disk stars in the solar neighborhood is $30\text{--}50\text{ km s}^{-1}$, as discussed for example in Mignard (2000, Table 6), and Alcobé & Cubarsi (2005, population components S_3 and A_3). At a distance $D \sim 9\text{--}10$ kpc, the above mechanism suffices to account for the peculiar velocity, and must have operated to some extent. It may have difficulty in producing a velocity perturbation of $70\text{--}80\text{ km s}^{-1}$, as would be the case if the source were at 6 or at 12 kpc.

3.2. Natal Kicks

We note that even at 9 kpc, the black hole possesses the momentum of a pulsar of $1.4 M_{\odot}$ with velocity of 530 km s^{-1} . Hence in the following we discuss the possible origin of the peculiar velocity in a natal supernova event, assuming one occurred. We examine this assumption in a later section.

3.2.1. Blaauw Kick

Mass unbound suddenly and symmetrically by the supernova explosion forces the binary to recoil with a momentum opposite to that of the unbound mass at the time of ejection. This spherical mass loss results in a kick that lies in the plane of the binary orbit. We estimate, using equation (1) of Nelemans et al. (1999), that mass unbound from the binary in a SN explosion imparted at most $23\text{--}44 \text{ km s}^{-1}$, for allowable mass ratios as measured by Greiner et al. (2001). Assuming the binary plane was randomly oriented, the kick has $\sim 25\%$ probability of lying in the galactic plane within $\pm 15^{\circ}$, which is the ratio of measured peculiar velocities perpendicular and parallel to the plane.

3.2.2. Asymmetric Kick:

If the binary lies at $D = 12 \text{ kpc}$ or 6 kpc , an *additional* kick of $\sim 30 \text{ km s}^{-1}$ is required. It is generally accepted that neutron stars form in asymmetric SN, and receive substantial birth kicks, which are seen in the velocities of young single pulsars, $\sim 400 \text{ km s}^{-1}$ (Hobbs et al. 2005). Neutron stars in long period binaries may receive smaller kicks of $\sim 50 \text{ km s}^{-1}$ (Pfahl et al. 2002), which is a case more closely related to the present binary with orbital period 33 days. This kick due to any asymmetries in the explosion has no preferred direction relative to the binary orbit plane, unless it is assumed that the progenitor’s spin is parallel to the orbital axis. Assuming random orientation, an asymmetric supernova has roughly the same 25% chance (as above), of producing a kick that lies in the Galactic plane.

3.3. Comparison with the kinematics of other black hole binaries

The question of whether or not black holes receive a natal kick similar to neutron stars is an open one. On the theoretical side, the formation of black holes of over $10 M_{\odot}$ challenges

stellar evolution models. Fryer & Kalogera (2001) proposed that black holes of that mass should form by direct collapse without SN explosion, or after a SN with energy insufficient to unbind the stellar envelope. Belczynski & Bulik (2002) also conclude that standard models would work only if wind mass loss for very massive stars was half as much as commonly assumed, and black holes of $\geq 10 M_{\odot}$ would form by direct collapse. Hence no kick velocity is expected in the formation of the most massive BH. There is some observational evidence that energetic SN may not occur in the formation of stellar black holes of relatively high mass. Cyg X-1 is a $10 M_{\odot}$ BH with a peculiar velocity of $< 10 \text{ km s}^{-1}$, and may be an example of such a ‘dark birth’ (Mirabel & Rodrigues 2003a).

Less massive black holes can form through partial fallback onto the collapsing object, after a SN explosion. We briefly evaluate the evidence for runaway black holes which have well measured, 3-dimensional velocities. The most likely mechanism for their high velocity is an asymmetric kick from a SN. Independent confirmation comes from rather difficult measurement of the supernova’s nucleosynthesis products in the companion star. Such evidence exists for neutron stars as well, e.g., González Hernández et al. (2005).

The runaway binary GRO 1655–40 contains a dynamically confirmed BH of $6.3 M_{\odot}$ (Greene et al. 2001), and has an anomalous velocity $v = 120 \text{ km s}^{-1}$ (Mirabel et al. 2002). Israelian et al. (1999) found super-solar abundances of several α -elements in the atmosphere of the companion star, and concluded that SN ejecta had enriched the companion. Foellmi et al. (2007), using different techniques, found little evidence for enrichment except in O. More recently, González Hernández et al. (2007), using VLT/UVES spectra, support the abundances derived by Israelian et al. (1999).

XTE 1118+48 is another confirmed $7\text{--}8 M_{\odot}$ BH binary (Gelino et al. 2006), orbiting in the Galactic halo with $v = 145 \text{ km s}^{-1}$. Mirabel et al. (2001) proposed that it was born in a globular cluster ~ 7 Gyr ago. However, more recently González Hernández et al. (2006) claim to have found fossil evidence of a supernova in the metal enrichment of the small mass donor, and propose instead that the progenitor was born in the Galactic disk and the binary shot out to the halo by the SN explosion.

LS 5039 has a runaway velocity of 126 km s^{-1} , (Ribó et al. 2002), and has clearly been kicked, but its mass estimate is closer to the neutron star range than the objects discussed above. It may contain a black hole of $3.7 M_{\odot}$ (Casares et al. 2005), if the binary is synchronized at periastron. Without the assumption of pseudo-synchronization, the mass might be as low as $1.4 M_{\odot}$. Regarding the direct detection of SN byproducts, McSwain et al. (2004) find N enrichment, but they caution that it could result from internal mixing due to rapid rotation, a scenario also favoured by Casares et al. (2005).

Finally, GRS 1915+105 does not fit easily in either the high or low speed category. The velocity is significantly higher than Cyg X-1. However, we cannot conclude that GRS 1915+105 is a runaway, because its low velocity out of the plane, and the operation of velocity diffusion in the plane, imply that any natal kick (symmetric and/or asymmetric) was probably smaller than $\sim 30 \text{ km}^{-1}$. We hope our data will permit an analysis such as done by Willems et al. (2005) for GRO J1655–40, who used all available information to reconstruct the evolution back to the time of core collapse and compact object formation. The observations, even for the small sample so far, imply a variety of formation scenarios for black holes.

4. Conclusions

1. The most massive known stellar black hole moves at $(53\text{--}80)\pm 8 \text{ km s}^{-1}$ with respect to its regional standard of rest, for any specific distance in the range 6–12 kpc.
2. At the distance of 9–10 kpc, the peculiar velocity is a minimum. If GRS 1915 is 3–5 Gyr old, it could have acquired this velocity by dynamic diffusion, i.e., non-circular motion imparted by perturbations such as spiral arms over time. In this case the black hole in GRS 1915+105 would have formed without a natal kick, like the $10 M_{\odot}$ black hole in Cyg X-1.
3. If the distance is smaller (6 kpc) or larger (12 kpc), then some additional $\sim 30 \text{ km s}^{-1}$ is required from another mechanism such as a natal supernova explosion, and the kick is constrained to lie within $\pm 15^{\circ}$ of the Galactic plane.

The National Radio Astronomy Observatory is a facility of the National Science Foundation operated under cooperative agreement by Associated Universities, Inc. V.D. acknowledges support from the Science Visitor’s Programme of the European Southern Observatory, Chile. M.R. acknowledges financial support from the Spanish Ministerio de Educación y Ciencia through a *Juan de la Cierva* fellowship linked to the project AYA2004-07171-C02-01, partially supported by FEDER funds. We thank Luis F. Rodríguez for helpful comments. This research has made use of NASA’s Astrophysics Data System and the **astro-ph** preprint service.

REFERENCES

Alcobé, S., & Cubarsi, R. 2005, A&A, 442, 929

- Beasley, A. J., & Conway, J. E. 1995, ASP Conf. Ser. 82: Very Long Baseline Interferometry and the VLBA, 82, 328
- Belczynski, K., & Bulik, T. 2002, ApJ, 574, L147
- Belloni, T., Klein-Wolt, M., Méndez, M., van der Klis, M., & van Paradijs, J. 2000, A&A, 355, 271
- Casares, J., Ribó, M., Ribas, I., Paredes, J. M., Martí, J., & Herrero, A. 2005, MNRAS, 364, 899
- Dehnen, W., & Binney, J. J. 1998, MNRAS, 298, 387
- Dhawan, V., Mirabel, I. F., & Rodríguez, L. F. 2000, ApJ, 543, 373
- Dhawan, V., Goss, W. M., & Rodríguez, L. F. 2000, ApJ, 540, 863
- Fender, R. P. 2003, MNRAS, 340, 1353
- Foellmi, C., Dall, T. H., & Depagne, E. 2007, A&ALetters(in press). arXiv:astro-ph/0702059
- Fryer, C. L., & Kalogera, V. 2001, ApJ, 554, 548
- Fuchs, Y., et al. 2003, A&A, 409, L35
- González Hernández, J. I., Rebolo, R., Peñarrubia, J., Casares, J., & Israelian, G. 2005, A&A, 435, 1185
- Gelino, D. M., Balman, Ş., Kızıloğlu, Ü., Yılmaz, A., Kalemci, E., & Tomsick, J. A. 2006, ApJ, 642, 438
- González Hernández, J. I., Rebolo, R., Israelian, G., Harlaftis, E. T., Filippenko, A. V., & Chornock, R. 2006, ApJ, 644, L49
- González Hernández, J. I., et al. 2007, A&A, submitted.
- Greene, J., Bailyn, C. D., & Orosz, J. A. 2001, ApJ, 554, 1290
- Greiner, J., Morgan, E. H., & Remillard, R. A. 1996, ApJ, 473, L107
- Greiner, J., Cuby, J. G., & McCaughrean, M. J. 2001, Nature, 414, 522
- Hobbs, G., Lorimer, D. R., Lyne, A. G., & Kramer, M. 2005, MNRAS, 360, 974
- Israelian, G., Rebolo, R., Basri, G., Casares, J., & Martín, E. L. 1999, Nature, 401, 142

- Johnson, D. R. H., & Soderblom, D. R. 1987, *AJ*, 93, 864
- Johnston, K. V., Spergel, D. N., & Hernquist, L. 1995, *ApJ*, 451, 598
- Kaiser, C. R., Gunn, K. F., Brocksopp, C., & Sokoloski, J. L. 2004, *ApJ*, 612, 332
- McSwain, M. V., Gies, D. R., Huang, W., Wiita, P. J., Wingert, D. W., & Kaper, L. 2004, *ApJ*, 600, 927
- Mignard, F. 2000, *A&A*, 354, 522
- Miller-Jones, J. C. A., Rupen, M. P., Fender, R. P., Rushton, A., Pooley, G. G., & Spencer, R. E. 2007, *MNRAS*, 375, 1087
- Mirabel, I. F., & Rodriguez, L. F. 1994, *Nature*, 371, 46
- Mirabel, I. F., Dhawan, V., Chaty, S., Rodriguez, L. F., Marti, J., Robinson, C. R., Swank, J., & Geballe, T. 1998, *A&A*, 330, L9
- Mirabel, I. F., Dhawan, V., Mignani, R. P., Rodrigues, I., & Guglielmetti, F. 2001, *Nature*, 413, 139
- Mirabel, I. F., Mignani, R., Rodrigues, I., Combi, J. A., Rodríguez, L. F., & Guglielmetti, F. 2002, *A&A*, 395, 595
- Mirabel, I. F., & Rodrigues, I. 2003, *Science*, 300, 1119
- Nelemans, G., Tauris, T. M., & van den Heuvel, E. P. J. 1999, *A&A*, 352, L87
- Pfahl, E., Rappaport, S., Podsiadlowski, P., & Spruit, H. 2002, *ApJ*, 574, 364
- Ribó, M., Paredes, J. M., Romero, G. E., Benaglia, P., Martí, J., Fors, O., & García-Sánchez, J. 2002, *A&A*, 384, 954
- Ribó, M., Dhawan, V., & Mirabel, I. F. 2004, *European VLBI Network on New Developments in VLBI Science and Technology*, 111
- Sellwood, J. A., & Binney, J. J. 2002, *MNRAS*, 336, 785
- Weilen, R., 1977, *A&A*, 60, 263
- Willems, B., Henninger, M., Levin, T., Ivanova, N., Kalogera, V., McGhee, K., Timmes, F. X., & Fryer, C. L. 2005, *ApJ*, 625, 324

Table 1. ICRF Position of Nucleus of GRS 1915+105.

MJD	RA	σ_{RA}	Dec	σ_{Dec}	Comment
50227	0.54975	1.8	0.7685	1.8	1996 May 24 / 8.4 GHz
50229	0.54970	1.8	0.7706	1.8	1996 May 26 / 8.4 GHz
50299	0.54965	1.5	0.7670	1.5	1996 Aug 03 / 8.4 GHz
50583	0.54955	1.5	0.7634	1.5	1997 May 15 / 8.4, 15 GHz
50744	0.54943	1.5	0.7621	1.5	1997 Oct 23 / 15 GHz
50752	0.54945	1.5	0.7629	1.5	1997 Oct 31 / 8.4 GHz
50913	0.54939	1.0	0.7589	1.0	1998 Apr 11 / 15 GHz
50935	0.54937	1.0	0.7582	1.0	1998 May 02 / 15 GHz
51331	0.54906	1.0	0.7522	1.0	1999 Jun 02 / 8.4, 15 GHz
51338	0.54905	1.0	0.7523	1.0	1999 Jun 09 / 8.4 GHz
52107	0.54870	0.8	0.7384	0.8	2001 Jul 17,18 / 8.4,15 GHz
52722	0.54846	0.5	0.7269	0.7	2003 Mar 24 / 8.4, 15 GHz
52731	0.54843	0.7	0.7265	0.9	2003 Apr 02 / 8.4, 15 GHz
52748	0.54840	0.5	0.7264	0.7	2003 Apr 19 / 8.4, 15 GHz
53794	0.54778	0.7	0.7093	0.8	2006 Feb 28 / 8.4 GHz
53800	0.54777	0.7	0.7095	0.8	2006 Mar 06 / 8.4 GHz

Note. — -

RA(J2000) offset in seconds from $19^{\text{h}}15^{\text{m}}11^{\text{s}}$.

σ_{RA} in milliarcseconds, i.e. multiplied by $\text{Cos}(\text{Dec})$

Dec(J2000) offset from $10^{\circ}56'44''$

σ_{Dec} in milliarcseconds.

Table 2. Velocity Components of GRS 1915+105 vs. Distance.

D	U	σ_U	V	σ_V	W	σ_W	UC	VC	VR _H	VT _H	VR _G	VC _G	V _P
5	122.9	7.5	-110.5	7.6	-1.1	1.8	127.8	-40.9	49.9	-116.2	-36.4	160.5	69.8
6	145.9	7.6	-133.2	7.7	-2.8	2.1	155.3	-64.2	52.7	-152.2	-42.1	164.5	69.7
7	168.9	7.7	-155.9	7.7	-4.4	2.5	178.6	-91.6	49.6	-188.0	-46.6	174.5	65.2
8	191.9	7.7	-178.6	7.8	-6.1	2.8	196.3	-120.7	41.3	-221.1	-49.7	189.9	58.4
9	214.9	7.8	-201.4	7.9	-7.7	3.2	208.3	-149.2	29.4	-249.6	-51.5	209.5	53.2
10	237.9	7.9	-224.1	8.0	-9.4	3.5	215.4	-175.4	15.8	-273.1	-52.3	232.1	54.5
11	260.9	8.1	-246.8	8.1	-11.1	3.9	218.9	-198.4	1.9	-291.8	-52.3	257.0	65.0
12	283.9	8.2	-269.5	8.2	-12.7	4.3	220.0	-218.2	-11.5	-306.4	-51.8	283.5	82.9
13	306.9	8.3	-292.2	8.3	-14.4	4.6	219.5	-235.0	-23.8	-317.9	-51.1	311.1	105.4
14	329.9	8.4	-315.0	8.5	-16.0	5.0	218.0	-249.2	-34.9	-326.8	-50.3	339.6	130.8
15	352.9	8.6	-337.7	8.6	-17.7	5.3	216.1	-261.3	-44.9	-333.9	-49.4	368.7	157.7

Note. — Column headings are:

1: D = Distance, kpc.

2–7: U, σ_U , V, σ_V , W, σ_W = Velocities transformed to LSR frame from the measured proper motion and errors. At each distance, σ_D is taken as 0. E.g., At 10 kpc, σ_U , σ_V , σ_W , are 8, 8, 4 km s⁻¹, from errors on μ_{RA} , μ_{DEC} , and V_{Helio} only.

8,9: UC, VC = Velocities (LSR), as expected from circular rotation at 220 km s⁻¹. WC = 0.

10: VR_H = Radial vel (Heliocentric), expected from circular rotation.

11: VT_H = Transverse vel (Heliocentric) across line of sight, expected from circular rotation.

12: VR_G = Measured radial vel (Galactocentric). 0 km s⁻¹ expected for circular rotation.

13: VC_G = Measured circular vel(Galactocentric). 220 km s⁻¹ expected for circular rotation.

14: V_P = Peculiar velocity = $[(U-UC)^2 + (V-VC)^2 + W^2]^{0.5} = [VR_G^2 + (VC_G - 220)^2 + W^2]^{0.5}$

Position of nucleus vs. time

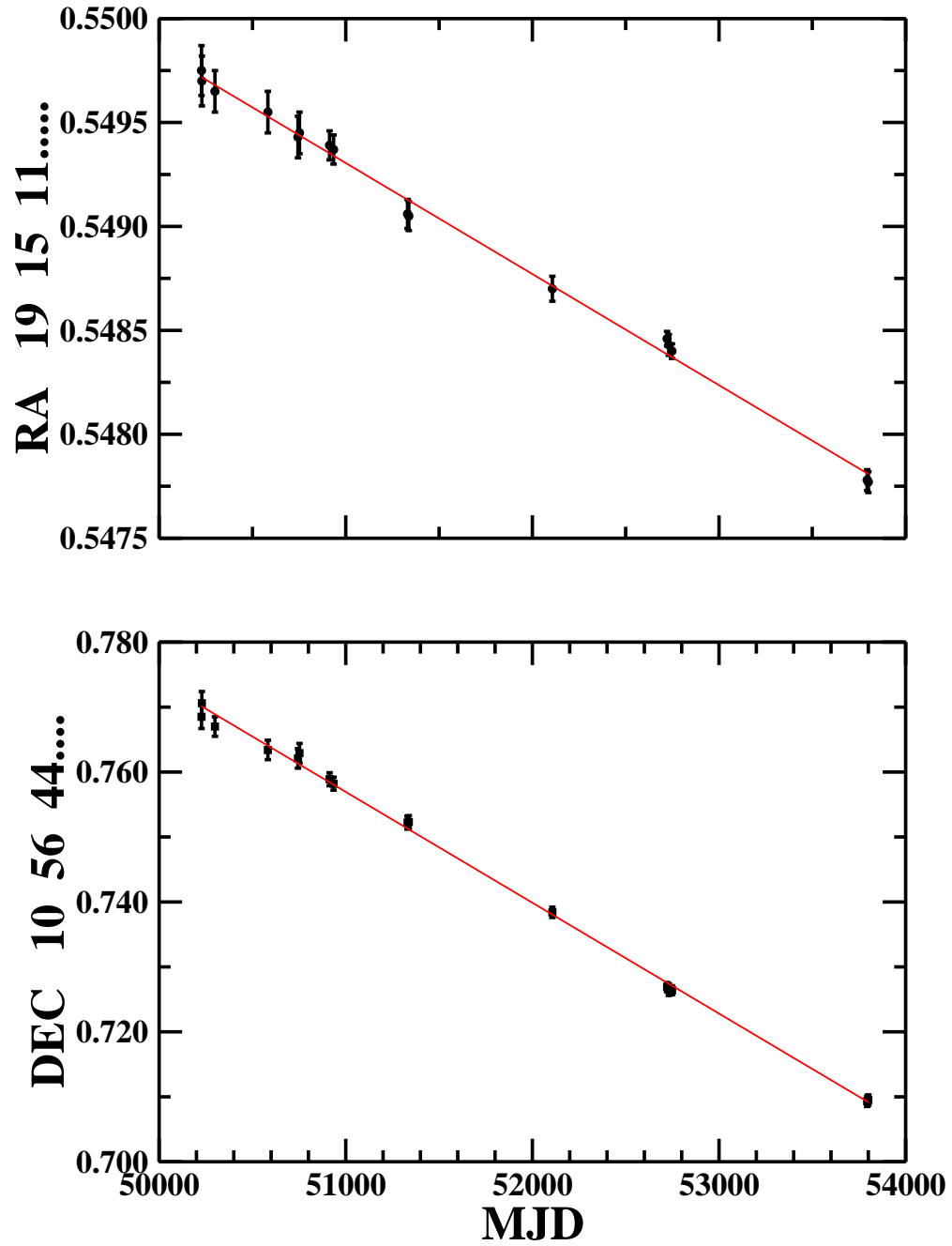


Fig. 1.— Astrometric Position of the Black Hole over a timespan of almost 10 years.

Velocity Components

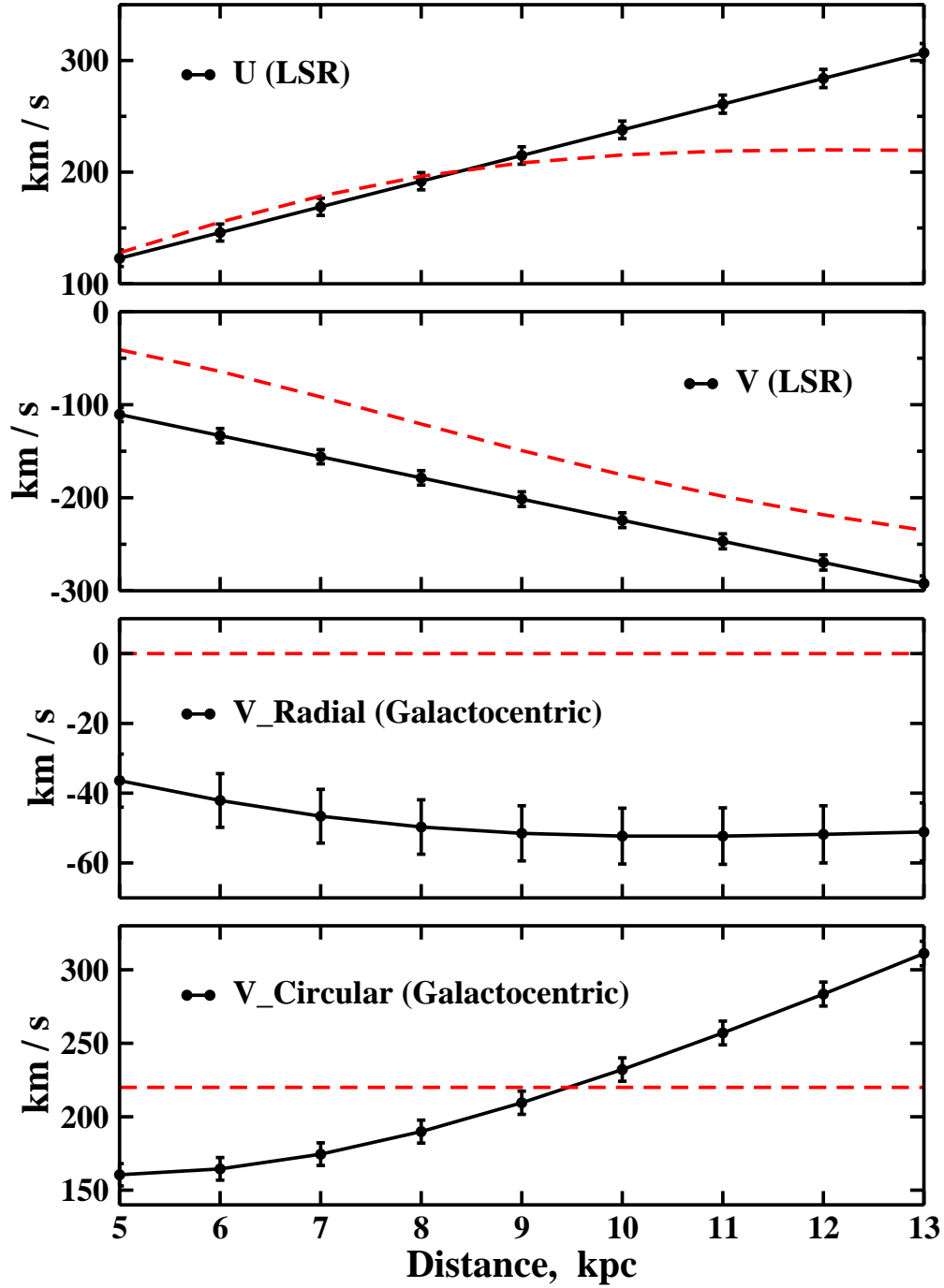


Fig. 2.— Measured velocity components (solid lines) vs. distance, compared with expected values for an object in circular rotation about the Galactic Center (dashed lines).

Total Peculiar Velocity of Black Hole

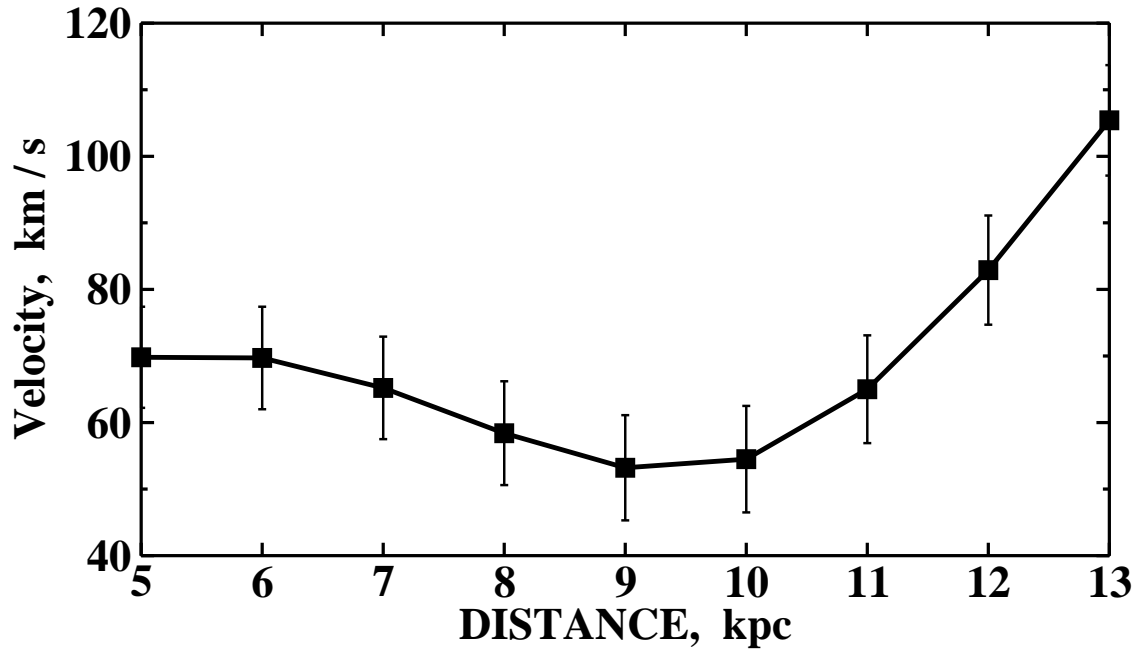


Fig. 3.— Total peculiar velocity of GRS 1915+105 plotted at various assumed distances.

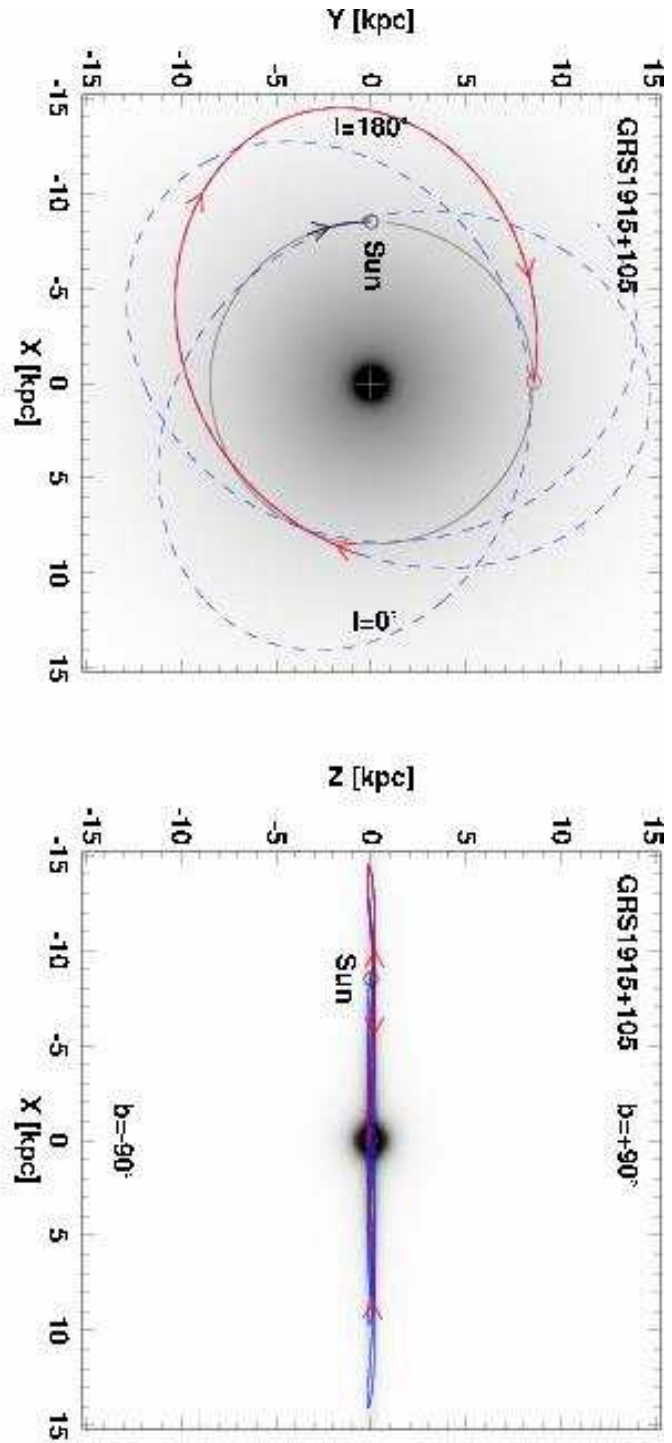


Fig. 4.— Galactocentric Orbit of GRS 1915+105 for the past 1 Gyr, (dashed blue line), with the most recent 250 Myr shown as the solid red line.